electronics

Review

A Survey on the State-of-the-Art and Future Trends of Multilevel Inverters in BEVs

Alenka Hren *,†, Mitja Truntič †and Franc Mihalič †

Faculty of Electrical Engineering and Computer Science, University of Maribor, Koroška Cesta 46, SI-2000 Maribor, Slovenia
* Correspondence: alenka.hren@um.si
† These authors contributed equally to this work.

Abstract: All electric vehicles are the only way to decarbonize transport quickly and substantially. Although multilevel inverters have already been used in some transportation modes, they are rarely used in road transportation, especially in light-duty passenger BEVs. With the transition to a high 800-V DC link to extend the driving range and enable extreme fast charging, the possibility of using multilevel inverters in commercial light-duty passenger BEVs becomes feasible. Higher efficiency, higher power density, better waveform quality, lower switching frequency, the possibility of using low-rated switches, and inherent fault tolerance are known advantages of multilevel inverters that make them an efficient option for replacing 2-level inverters in high DC link passenger BEVs. This paper discusses high DC link voltage benefits in light-duty passenger BEVs, presents the state-of-the-art of different conventional multilevel inverter topologies used in BEVs, and compares them with conventional 2-level inverters from different aspects and limitations. Based on commercial upper-class passengers' BEV data and a review of multilevel inverters on the market, future trends and possible research areas are identified.

Keywords: multilevel inverters (MLI); electric vehicle (EV); passengers' battery electric vehicle (BEV); extreme fast charging (XFC); higher voltage batteries; WBG semiconductors

Citation: Hren, A.; Truntič, M.; Mihalič, F. A Survey on the State-of-the-Art and Future Trends of Multilevel Inverters in BEVs. *Electronics* **2023**, *12*, 2993. https://doi.org/10.3390/electronics12132993

Academic Editors: Sergio Busquets-Monge and Fabio Corti

Received: 17 May 2023
Revised: 4 July 2023
Accepted: 6 July 2023
Published: 7 July 2023

1. Introduction

Personal mobility plays a crucial role in human society, serving as a highly valued aspect that is essential for both the productive functioning of the economy and individuals' ability to access necessary opportunities for personal growth. The technologies and systems enabling widespread personal mobility offer substantial benefits that should not be underestimated. However, as accessibility and the range of mobility options increase, concerns about the long-term sustainability of our transportation systems also arise.

Currently, many transportation modes possess a significant physical presence, consume substantial amounts of energy resources, and contribute significantly to anthropogenic greenhouse gas emissions as well as local air, noise, and water pollution. It is imperative to address these issues to foster a more sustainable and environmentally friendly approach to personal mobility.

Electrification of transportation systems has been recognized and considered the most promising solution for many issues caused by greenhouse gas emissions. Nowadays, transportation systems contribute more than 20% of the total greenhouse gas emissions worldwide, while in the EU they account for more than 25% [1]. In addition to reducing greenhouse emissions, electrification of transportation systems can also lead to higher energy efficiency, less required maintenance of vehicles, and better acceleration, which are seen as important advantages of electric vehicles (EVs) when making purchase decisions. Furthermore, EVs have the capability to directly utilize energy derived from renewable sources. When EVs are connected to the power grid, their batteries can play a crucial role in stabilizing the grid by balancing supply and demand, thereby facilitating the seamless

integration of renewable energy sources. In addition, the adoption of electricity as a means of transportation is expected to make a significant contribution to enhancing the security of the energy supply.

By utilizing electricity for transportation, EVs not only increase the energy efficiency of vehicles, but they also bring about a diversification of energy sources in the transport sector. This becomes particularly important due to the persistently unstable political situation in many countries that export oil and gas. Such instability is expected to lead to future fluctuations in oil prices. Therefore, the ability to rely on alternative energy sources for transportation, such as electricity, becomes crucial in mitigating the potential impacts of these oscillating oil prices.

On the other hand, the limited maximum driving range and long charging time compared to the fuel refilling time of a gasoline-powered internal combustion engine (ICE) are the main drawbacks of EVs, especially plug-in battery electric vehicles (BEVs).

To meet EU sustainable and smart mobility strategy targets of at least 30 million zero-emission vehicles in operation on European roads and 100 climate-neutral European cities by 2030 [2], it is anticipated that a significant improvement in battery performance is required with respect to increasing the driving range of BEVs and the rate at which they can be recharged, along with the requirement that the cost of the purchase and ownership of BEVs must be comparable with the cost of internal combustion engine vehicles (ICEV). The industry is making significant progress in addressing the last requirement. Tesla has already cut BEV costs by 50% when comparing the flagship Model S and Model X to the newer Model 3 and Model Y. They announced that with the upcoming next-generation BEV platform, the costs will be further reduced. While the recent advances in battery production and their cost drops have led to the usage of battery packs of larger capacity, enabling improvements in the driving range of BEVs based on a single recharge, fast charging remains a major challenge [3].

A comparison between different light-duty passengers' BEVs and ICEVs in terms of the required travel times for an 845 km inter-city distance is presented in [4]. The required travel time concerning the battery capacity heavily depends on the BEV's maximum driving range, influencing the number of recharging stops and the time needed to recharge the battery. It is demonstrated that chargers of more than 400 kW are needed to have comparable travel times between EVs and ICEVs based on the current capacities of batteries. As a possible solution to this issue, the use of extremely fast chargers (XFCs) is proposed in [5,6].

Recently, many leading car manufacturers have started BEV production with higher DC links in traction drives or have announced this transition very shortly. For some commercial upper-class passengers' BEVs on the market and announced new releases, the data given in Tables 1 and 2 were obtained from the Electric Vehicles Database [7], which among many open-access databases on EVs offers the most comprehensive and up-to-date overview of all current and past electric vehicles. While Table 1 summarizes data on the DC voltage system, nominal and usable (value is given in parentheses) battery capacity, and production year, Table 2 summarizes data on the estimated efficiency, fast charge speed, and maximum fast charge power, along with the estimated average charge power over the 10% to 80% range of battery state-of-charge (SoC) for some commercial upper-class passengers' BEVs (in parentheses). It is important to note that the car's manufacturers provide fast charge speeds in terms of kilometers per minute (km/min) rather than kilowatts per minute because it gives drivers a more intuitive understanding of how fast the charging is, and additionally, it allows more accurate comparisons between different charging systems and vehicles. Fast charging speed is strongly connected with the average fast charge power, estimated efficiency, and battery capacity.

Table 1. DC voltage system of some BEVs on the market and announced new releases.

Vehicle	Production Year	DC Voltage (V)	Nominal and Usable Battery Capacities (kWh)
Mercedes EQS 450+	2021	400	120 (107.8)
NIO ET5	2022	400	100 (90)
Tesla S Dual Motor	2023	400	100 (95)
Porsche Taycan 4S Plus	2020	800	93.4 (83.7)
Audi e-tron GT RS	2021	800	93.4 (85)
KIA EV6 Long Range	2021	800	77.4 (74)
Hyundai IONIQ 6 LR AWD	2022	800	77.4 (74)
Genesis GV60 Premium	2022	800	77.4 (74)
BYD HAN	2023 (from March)	800	85.4 (83)
Lucid Air Pure	2023 (from June)	800	88 (88)
XPENG G9 AWD	2023	800	98 (94)

Table 2. Estimated efficiency, fast charge speed, and maximum fast charge power for some BEVs on the market and announced new releases.

Vehicle	Estimated Efficiency (Wh/km)	Fast Charge Speed (km/min)	Max. and Average Fast Charge Powers (kW DC)
Mercedes EQS 450+	170	15.8	207 (173)
NIO ET5	180	8.7	140 (100)
Tesla S Dual Motor	165	13.2	250 (140)
Porsche Taycan 4S Plus	182	18.8	268 (216)
Audi e-tron GT RS	210	16.7	268 (216)
KIA EV6 Long Range	180	17.8	233 (200)
Hyundai IONIQ 6 LR AWD	149	19.2	233 (200)
Genesis GV60 Premium	190	17	233 (200)
BYD HAN	178	7.5	120 (85)
Lucid Air Pure	157	16.3	200 (160)
XPENG G9 AWD	214	15.3	300 (210)

As seen from Table 1, several manufacturers are migrating from current 400 V-based systems to ones with an 800-V rating. In addition to improving charging performance and efficiency, higher voltage systems allow battery recharge to be completed in a much shorter time, meaning that significantly lower charging currents can be utilized, resulting in less heat generation and possibly reduced energy loss. Consequently, more usable energy can be retained, and the vehicle travel range between charges will be significantly extended. Regardless of whether lower currents result in lower conduction losses, the total efficiency is not necessarily reduced because higher voltages cause higher switching losses when the same inverter technology is employed [8]. Due to the 650-V switch blocking voltage limitation, a conventional 3-phase six-switches 2-level inverter, shown in Figure 1, is unsuitable for applications with an 800-V DC link voltage. Therefore, either the semiconductors or the inverter topology must be changed. High-voltage semiconductor production involves higher costs, and their usage results in higher switching losses. Therefore, using a multilevel inverter (MLI) appears to be a more promising and possible solution.

As added value to the comprehensive review of MLI in EVs [9], in this paper it is first shown and confirmed by collected data that the introduction of high 800-V systems, a significant step from existing 400-V systems, is happening faster than predicted in upper-class passengers' BEVs because it allows them to become more competitive with ICEVs in intercity driving. Moreover, the purpose of the paper is to evaluate the importance of power inverters for EV motor drive systems and, since the first implementations are already on the market, to highlight and confirm the strong potential of MLIs to replace the conventional 2-level inverter in upcoming new releases of light-duty passenger BEVs.

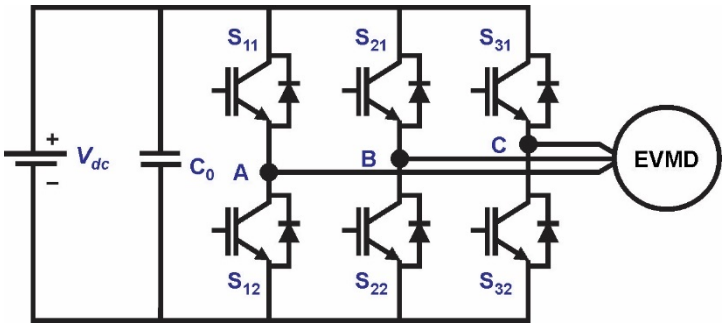

Figure 1. Conventional 2-level, 3-phase VSI topology for electric vehicle motor drive.

The remaining paper is structured as follows: The benefits of high DC link voltage in light-duty passengers' BEVs are discussed in Section 2. Section 3 is dedicated to a comprehensive overview of classical MLI topologies, followed by a comparative study of CHB and NPC MLI topologies with conventional 2-level inverters in Section 4. The state-of-the-art of MLIs in different transportation modes is presented in Section 5, and finally, the paper's conclusions are given in Section 6.

2. High DC Link Voltage Benefits Light-Duty Passenger BEVs

Several EV manufacturers have either already adopted or are planning to adopt an 800-V DC link for their latest passenger electric vehicles. This shift can be observed from the data provided in Table 1 and is primarily driven by the potential to extend the driving range of vehicles and facilitate the use of high-speed chargers. However, the advantages of employing an 800-V DC link extend far beyond these benefits. Switching to an 800-V DC link results in various advantages, including lighter cables, reduced weight and energy losses, lower manufacturing costs, higher power density, and more efficient motors [10]. Many experts in the industry believe that advancements in boosting the electrical systems of passengers' BEVs to an 800-V DC link, departing from the current industry standard of a 400-V DC link, could serve as a significant breakthrough. This transition has the potential to enhance the competitiveness of EVs and eventually lead to their widespread adoption, potentially replacing combustion vehicles. This shift to an 800-V DC link is considered a necessary transition as Europe, along with other regions, aims to reduce vehicle emissions and address the challenges of climate change.

2.1. BEV Battery Pack and Battery Management

A BEV battery pack is a very important and expensive component of BEV and presents one of the main barriers because people are reluctant to switch from fossil fuel to battery power. It consists of many individual lithium-ion cells connected in series or parallel combinations. Each cell operates over a voltage range of 3.1 to 4.2 V. For a nominal 800-V system, there are approximately 198 cells in series, giving an overall pack voltage of 610 to 835 V.

For a better understanding of the different voltage-level battery systems in the EVs within the 400-V and 800-V systems, Table 3 presents the number of included cells with pack configuration and the battery's nominal voltage. Based on available information in the Electric Vehicle Database [7], most lithium-ion batteries are mixed metal oxides like the NCM type (Lithium Nickel Cobalt Manganese) and a few NCA types (Lithium Nickel Cobalt Aluminum) or LFP types (Lithium Iron Phosphate) of used materials for the cathode. For example, the Mercedes EQS 450+ uses for the cathode a molar composition of 80% nickel, 10% cobalt, and 10% manganese, abbreviated as NCM811, and has the formula $LiNi_{0.8}Mn_{0.1}Co_{0.1}O_2$. To achieve higher energy density and operating voltage, optimization of the NCM structure is a permanent concern during manufacturing. Due to the ethical problems with cobalt mining and the metal's high cost, reducing cobalt content is essential. Nevertheless, within the listed EVs in Table 3, from the available information

for the cathode materials, there are five NCM (Audi, Mercedes, NIO, Porche, and XPENG), one NCA (Tesla), and one LFP (BYD) type.

Table 3. The number of cells, pack configuration, and battery's nominal voltage.

Vehicle	Number of Cells	Pack Configuration	Battery Nominal Voltage (V)
Mercedes EQS 450+	432	108s4p	396
NIO ET5	96	96s1p	no data
Tesla S Dual Motor	7920	110s72p	407
Porsche Taycan 4S Plus	396	198s2p	725
Audi e-tron GT RS	396	198s2p	725
KIA EV6 Long Range 2WD	384	192s2p	697
Hyundai IONIQ 6 LR 2AWD	384	192s2p	697
Genesis GV60 Premium	384	192s2p	697
BYD HAN	178	178s1p	569
Lucid Air Pure	No data	No data	No data
XPENG G9 AWD	No data	No data	No data

Each car manufacturer has decided on a specific battery pack configuration based on the required number of cells in series and parallel. Table 3 shows each car's battery pack configuration with a particular number of series and parallel lithium-ion cells to ensure the required battery capacity in kWh: from 96 cells and up to 400 cells, only Tesla uses almost 8000 cells. The battery's nominal voltages (when available) are also listed within the rated DC voltage systems in Table 3.

Initially, it may appear that increasing the battery pack voltage to 800 volts would have a minimal impact on the pack itself. However, there are several considerations and challenges that need to be addressed. One prominent concern is safety, as higher battery voltages increase the risk of electric shock if someone unintentionally becomes part of the battery circuit. Moreover, higher voltages are more likely to initiate an arc, necessitating a greater separation distance for the arc to be extinguished. This particularly affects the design of fuses in the battery circuit, as higher voltages require specific techniques, such as increased separation distance or the use of non-conductive materials to suppress any arcs, thereby significantly increasing the cost of the fuse. Another issue arises from the impact of high currents within a battery pack on various components, such as busbars, disconnect switches, and tabs, resulting in elevated costs and added weight to the battery pack. Additionally, the capacity of a battery, measured in ampere-hours (Ah), is limited by its weakest cell. This concern is less significant for packs comprising multiple lower-capacity cells connected in parallel and then in series, as opposed to packs made up of single large-format cells connected in series. Lastly, an often-overlooked issue is the increase in leakage currents from the battery to the chassis as pack voltage rises. This factor needs to be taken into account, as it can have implications for the overall system.

As battery thermal management and cooling system issues must also be addressed and solved to enable XFC, it is predictable that future battery management will involve higher costs and complexity [11].

2.2. Charging Stations and Extremely Fast Charging (XFC)

One of the main objectives of transitioning to a higher DC-link voltage in BEVs is to enable fast charging. Fast charging can help promote market penetration by improving the utility of EVs or the travel destinations of BEVs, thus improving range limitations, often cited by consumers as a barrier to adopting EV technology.

The actual installed charging station infrastructure can be classified into two different classes. Commonly used today is an AC infrastructure with an available power of up to 22 kW, depending on the local or national infrastructure. In this case, an BEV is charged by an internal charger that connects the internal DC link with the external AC voltage of the infrastructure. A fast-charging infrastructure has also been rapidly built in the last few

years. A direct DC connection between the charging infrastructure and the internal BEVs DC link is used in this case. The charging infrastructure equipment continuously operating above 150 kW and ensuring the battery's recovery from 10% to 80% within 15 min (or to refill range at a rate of ~20 miles per minute of charge) is considered XFC [5,6]. Again, Table 4 summarizes obtained data from the Electric Vehicle Database [7] on 10% to 80% range estimation, average fast charge power, and time to charge the battery from 10% to 80% SoC, all related to fast charge speed (see Table 2).

Table 4. The 10% to 80% range estimation, time to charge from 10% to 80% SoC, and average fast charge power for some BEVs on the market and announced new releases.

Vehicle	10% to 80% Range Estimation (km)	Time to Charge from 10% to 80% (min)	Average Fast Charge Power (kW DC)
Mercedes EQS 450+	64–508	28	173
NIO ET5	50–400	40	100
Tesla S Dual Motor	58–460	30	140
Porsche Taycan 4S Plus	46–368	17	216
Audi e-tron GT RS	41–324	17	216
KIA EV6 Long Range	48–328	16	200
Hyundai IONIQ 6 LR AWD	39–312	16	200
Genesis GV60 Premium	39–312	16	200
BYD HAN	47–372	43	85
Lucid Air Pure	56–448	24	160
XPENG G9 AWD	44–352	20	210

Apparently, all the times to charge the battery from 10% to 80% SoC are longer than 15 min, so none of the BEVs in question currently support XFC as defined. As the charging rate depends on the charger used (up to 350 kW) and the maximum charging power the BEV can handle, enabling XFC can be obtained by increasing the power of both, or at least by increasing the BEV's maximum charging power. Infrastructure and economic considerations related to the effective implementation of fast charging above 400 kW are discussed in [12].

While the rapid expansion of fast and high-speed charging stations brings significant benefits to BEV drivers, it also presents challenges on the grid side. These challenges include high monthly demand charges due to peak power draws and the potential requirement for costly grid reinforcements. To address these issues, the use of Stationary Energy Storage (SES), such as batteries, at the charging station or the integration of Renewable Energy Sources (RESs) can help mitigate grid-related challenges. A comprehensive examination of the advantages and challenges associated with energy storage at fast-charging stations, as well as a detailed discussion of various power electronic architectures utilizing batteries, flywheels, and hydrogen energy storage, can be found in [13,14].

However, when considering a charging station design with battery storage for a 400-V DC link BEV, the implementation becomes relatively straightforward. The stationary battery can be configured to have a minimum voltage slightly higher than the maximum voltage of the BEV battery.

On the contrary, when a charging station equipped with battery storage needs to cater to both 400-V and 800-V DC link BEVs for fast charging, the design complexity increases. Since the stationary battery has a predetermined voltage range, the isolated DC/DC converter that connects the stationary battery to the BEV battery must be designed with a wide output voltage range. In such scenarios, it is essential to conduct system optimization to determine the optimal voltage range for the stationary battery, considering the specifications of the DC/DC converter. Consequently, the design approach for fast and high-speed charging stations with stationary energy storage should be strategic to ensure efficient charging for 800-V DC-link BEVs.

In the context of XFCs, the primary objective is to recharge the EV battery to 80% capacity within a timeframe of 15 min, which is comparable to the refueling time for ICEVs. This requires charging powers of 350 kW or more, necessitating the output voltage range of XFC stations to be within 800–1000 V. Current XFC chargers can provide up to 400 A, delivering a total power of 240 kW. However, advanced XFC chargers under development

aim to offer up to 500 A at 1000 V, providing a total power of 500 kW. Typically, a BEV battery can be charged in approximately 80 min using a 50-kW charger, providing a travel range of 400 km. However, the limitations of connectors and cabling pose challenges for widespread deployment of XFC technology. Existing connectors can handle a continuous current of up to 200 A, limiting the charging power to 160 kW in an 800-V system and requiring a charging time of around 25 min to support a 400 km travel range. Higher-voltage battery packs are crucial for XFC, and liquid-cooled connectors capable of handling currents up to 350 A are required. The liquid-cooled connectors are already available and can support a charging time of 15 min for a 400-kilometer travel range, which is comparable to the refueling time for ICEVs.

While the growth of BEVs and XFC stations has a positive environmental impact, it can also pose challenges to the AC power grid. Increased peak demand, voltage instability, reduced reserve margins, and reliability are some of the challenges associated with high charging loads. To address these issues, a sustainable and grid-independent DC power network is proposed in [15]. The network relies on photovoltaics (PV) and a co-located lithium-ion battery storage system (BESS) to enable high-speed charging. Evaluation of the network's power savings for different voltage use cases (low, medium, and high) shows an improvement of 17% to 25% compared to the AC power grid case.

2.3. Copper and Cables

Copper is a fundamental component of the BEV revolution, playing a crucial role in three key areas of electrical transportation growth: energy storage, charging infrastructure, and BEV production. The utilization of copper in BEVs is driven by its cost-effectiveness, high durability, malleability, and conductivity. On average, EVs require up to four times more copper compared to conventional ICEVs [16]. An average ICEV necessitates 20 kg of copper; hybrid electric cars require 40 kg; and BEVs require as much as 370 kg of copper per vehicle. In addition to its application in BEV manufacturing, copper also holds significance in EV infrastructure. Wood Mackenzie, a global research and consulting firm for the natural resources industry, estimates that the EV sector will require 250% more copper by 2030 solely for charging stations. This forecast takes into account the expectation of over 20 million EV charging points worldwide. A single charging station alone contains approximately 8 kg of copper for a 200-kW charger.

The DC link voltage in a BEV significantly influences the amount of copper used. One notable advantage of higher-voltage systems is their impact on the connection of various electric components. Assuming a constant power level, an 800-V system requires half the current compared to a 400-V system, enabling a reduction in the cross-section of the wiring harness due to decreased current requirements. For instance, at a steady-state current of 250 A in a 400-V system, a wiring harness with a cross-section of 95 mm^2 is needed. In contrast, a reduced steady-state current of 125 A in an 800-V system requires a cross-section of 35 mm^2. This reduction in cross-section results in a decrease in copper weight from approximately 0.85 to 0.31 kg/m, representing a factor of 2.7. Additionally, the smaller cross-section of the wiring harness allows for increased flexibility in routing, leading to a reduction in vehicle volume. Lower current levels also have positive effects on the design of the high-voltage (HV) battery. Battery cells are typically assembled into modules comprising ten to fifteen cells. Thermal losses in cell and module connections contribute significantly to cell heating. By reducing the current by a factor of two, the copper losses at the same cross-section of the bus bar are reduced by a factor of four. With careful selection of wiring design, module connectors, and bus bars, substantial weight savings can be achieved. Furthermore, a reduction in vehicle weight optimizes consumption and efficiency. Additionally, the decrease in copper quantity reduces the material cost of the wiring harness and bus bars, although there are additional material costs associated with HV packs due to the doubling of channels in the battery management system.

Another consideration is the weight of the cables connecting the charger to the BEVs. Occupational Safety and Health Administration regulations specify a maximum cable

weight of 22.7 kg for a single person to handle. In the case of an 800-V XFC system, the cable weight exceeds the safety limit for a 350-kW charger when assuming a cable length of 1.85 m [9,12]. However, adopting a 1 kV DC voltage would satisfy the safety limit for the same power level.

2.4. Electric Motors

Designing electric motors for BEVs involves high effort because high specific torque, low noise, fast dynamic response, low torque at high speeds, low cost, overload capability, fault tolerance, high mechanical robustness, and ruggedness are required, with a focus on high starting torque to meet acceleration requirements, high efficiency to extend the range, and high power density to reduce motor volume.

Electric motor motion relies on the interaction of the rotor magnetic field and a rotating magnetic field generated by time-controlled currents in the stator windings. As the motor operating voltage increases for a given input power, the input RMS current is reduced, and consequently, the stator winding copper losses are reduced. Losses are typically reduced by a factor of four using an 800-V versus a 400-V supply.

This offers the opportunity to reduce the copper winding wire diameter, which decreases the overall volume and increases the packing efficiency, allowing for smaller motors. The same lower current requirements in an 800-V system reduce not just the motor copper losses but losses in the entire system wiring loom, introducing weight, space, and cost savings.

The utilization of 800 V voltage enables electric motors to operate at speeds up to 20,000 rpm, which is significantly higher than the speed achievable by 400-V electric motors. As a result, these motors exhibit improved power density. This implies that they efficiently convert electrical power into mechanical power at high speeds rather than high torque. Typically, motor size is determined by its torque capability. Therefore, this characteristic allows for the utilization of much smaller motors. In fact, smaller high-speed motors can weigh as little as 25 kg, thereby reducing the overall weight of a vehicle. This reduction in weight enables the vehicle to travel considerably further on a single charge.

3. Multilevel Inverters

MLIs are undoubtedly state-of-the-art in applications with high power and high voltages (e.g., electric power plants) or in applications that require good-quality sinusoidal currents (e.g., photovoltaic inverters) [17]. With the trend of higher voltages and power demand in automotive electric drivetrains, the advantages of MLI, such as higher efficiency, higher power density, better waveform quality, lower switching frequency, the possibility of using low-rated switches, and inherent fault tolerance, become valuable for automotive main traction drives. The significant demand for power components that comes with the electrification of the automotive industry will continue to grow for the next few decades. Parallelly, the efficiency of battery energy usage is critical for the cost and performance of electric cars, and wide bandgap (WBG) Gallium-Nitride (GaN)-based components, which are superior to competing technologies, are undermining the long reign of silicon in the power world.

The fundamental operational principle of MLI involves generating a stepped output voltage waveform that approximates a sine shape, enabling higher voltage and power levels to be achieved. The MLI's structure typically comprises one or more DC sources and an array of low-rate power semiconductor switches. By increasing the number of voltage levels in the output waveform and employing an appropriate switching strategy, it becomes possible to generate an almost sinusoidal output voltage without the need for bulky transformers and passive filters. Regarding their structure, conventional MLIs can generally be categorized into three main types: neutral point clamped (NPC), flying capacitor-based (FC), and cascade H-bridge (CHB). Their basic, well-established topologies have been extensively analyzed [18–21] and documented, and they have been commercially used for more than two decades.

Speaking of MLI, more sinusoidal currents (lower total harmonic distortion (THD)) reduce harmonic losses in the electric motor, support the noise, vibration, and harshness (NVH) characteristics of the electric drivetrain, improve the EMC behavior, and therefore also reduce the stimulation of bearing currents. The lower THD is achieved by utilizing additional voltage levels in the output voltage of the MLI when compared to the standard 2-level type inverter. However, despite the numerous advantages of MLIs, they also come with certain drawbacks. These include the requirement for voltage balancing, a higher number of semiconductor switches and capacitors, and a more complex control system.

3.1. Cascade H-Bridge MLI

The concept of MLI technology appeared in the 1970s with the introduction of the multilevel stepped waveform generated with a series-connected H-bridge, which is also known as a cascaded H-Bridge converter (CHB). In the last two decades, several companies have commercialized it, and it is suitable for FACTS and motor drive applications. The topology of a 3-phase, 5-level CHB is shown in Figure 2.

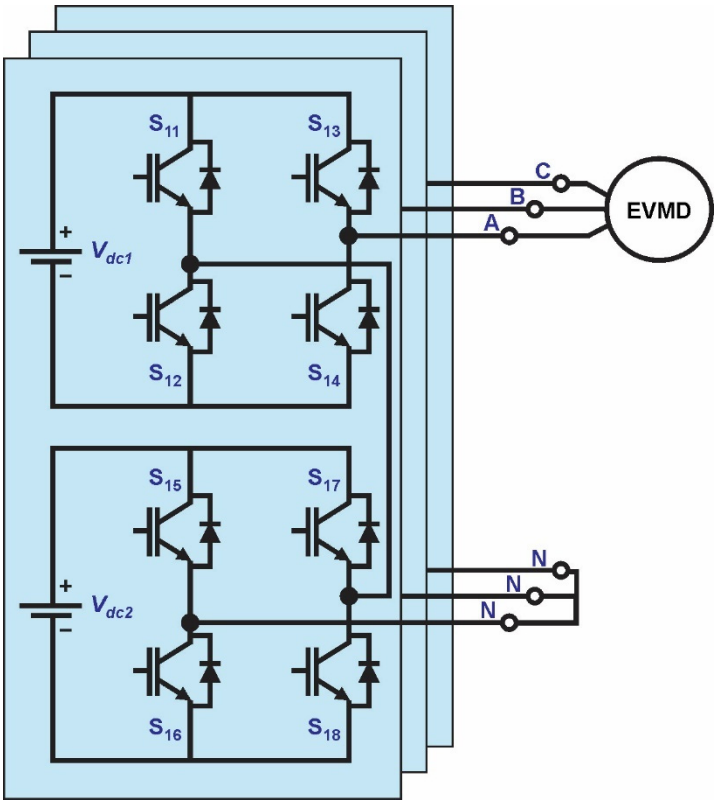

Figure 2. Topology of a 3-phase, 5-level CHB MLI.

The main features of CHB topology are its modular structure realized by simple power cell (H-bridges) serial connection, allowing fault-tolerant operation with added bypass switches, and straightforward extension by using a large number of series connecting cells, resulting in a large number of levels in the generated high nominal output voltage. Generally, when n H-bridges are serially connected, the $2 \times n + 1$ voltage levels are obtained in the inverter output voltage at the lowest component count when compared to FC and NPC MLI topologies. Equalization of losses, equal power distribution, and improved quality of the output voltage waveform can be achieved by applying a well-known phase-shifted pulse-width modulation (PWM) technique. Since each H-bridge requires an independent DC source, this can be seen as the main topology drawback, limiting its suitability for some applications. For proper comparison of MLI inverter

topologies, the allowed switching states and output voltage levels for 3-level CHB MLI are given in Table 5.

Table 5. A 3-level CHB MLI allows switching states and output voltage levels.

Switching States	S_{11}	S_{12}	S_{13}	S_{14}	Output Voltage
1	1	0	0	1	V_{dc}
2	1	0	1	0	0
3	0	1	0	1	0
4	0	1	1	0	$-V_{dc}$

Since output voltage zero level can be generated by connecting the inverter output either to the positive or negative inverter bars, this redundancy can be exploited to enable fault-tolerant operation. When more H-bridges are serially connected, the redundancy inherently increases as each H-bridge has one redundant switching state.

3.2. NPC MLI

Eventually, in the late 1970s, the concept of the diode-clamped converter (DCC) emerged. Over time, it transformed into the three-level Neutral Point Clamped (3-level NPC MLI) inverter that we are familiar with today. A 3-phase, 3-level NPC, shown in Figure 3, was first proposed in [22]. The presented results of an analytical and experimental comparison between an NPC PWM-based MLI and a conventional 2-level inverter confirm its excellent drive system efficiency and suitability for a wide-range variable speed operation. Since then, it has been the topic of numerous research projects in academia and industry, to name a few [23–26].

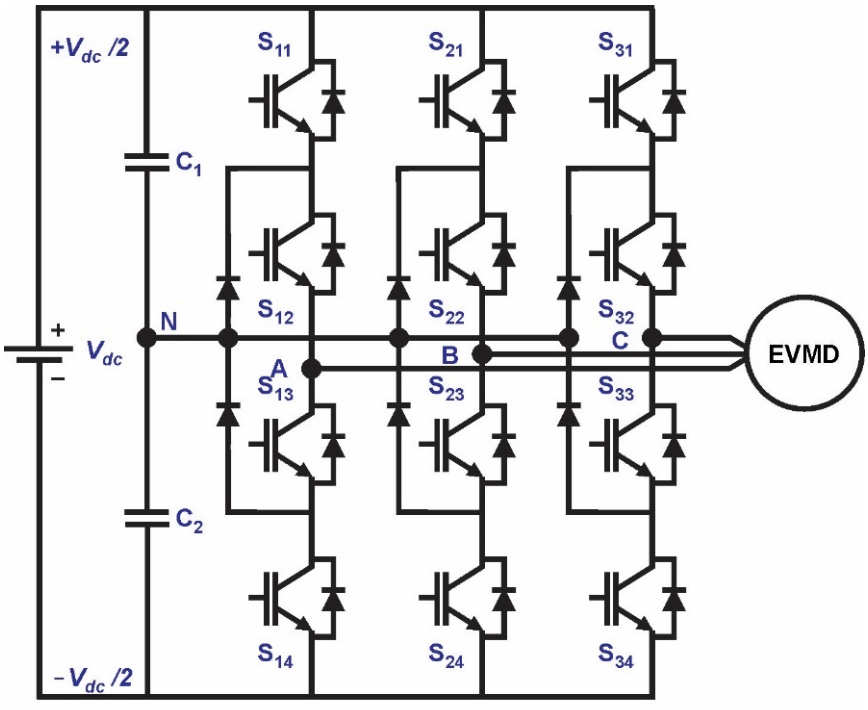

Figure 3. Topology of a 3-phase, 3-level NPC MLI.

This topology consists of three legs, where in each inverter leg, two conventional 2-level inverters with the midpoint of the transistors connected to neutral point N by two clamping diodes enable the generation of an additional zero voltage level in the inverter output voltage. Taking first-leg operation as an example, the allowed switching states and corresponding output voltage levels are given in Table 6.

Table 6. A 3-level NPC MLI allows switching states and output voltage levels.

Switching States	S_{11}	S_{12}	S_{13}	S_{14}	Output Voltage
1	1	1	0	0	$V_{dc}/2$
2	0	1	1	0	0
3	0	0	1	1	$-V_{dc}/2$

As each semiconductor device must block just half of the inverter input DC voltage, switches with lower voltage ratings can be adopted, or when the same switches are used, the inverter power rating can be doubled with respect to 2-level inverters.

This development marked the introduction of a multilevel power converter specifically designed for medium-voltage applications. For more than two decades, many companies have successfully commercialized this technology, primarily for medium-voltage applications, such as Flexible AC Transmission Systems (FACTS) and motor drives. The key advantage of the 3-level NPC inverter lies in its topology, where clamping diodes are incorporated to equalize the blocking voltages across the semiconductor power switches. By employing a simple PWM level-shifted multicarrier modulation strategy with added zero-sequence injection, DC voltage imbalance control can be achieved.

The main NPC MLI disadvantage appears to be an unequal distribution of the losses between semiconductor switches, leading to unequal temperature distribution and setting limits on inverter output power. To overcome this drawback, the active NPC MLI topology shown in Figure 4 has been proposed. In this topology, the clamping diodes are replaced by active semiconductor switches, allowing the application of an appropriate modulation strategy to assure evenly distributed power loss between semiconductor switches, subsequently improving the inverter terminal characteristics [27–31]. The distribution of power loss can be controlled only during the output zero-voltage level, as this can be achieved in four different switching states.

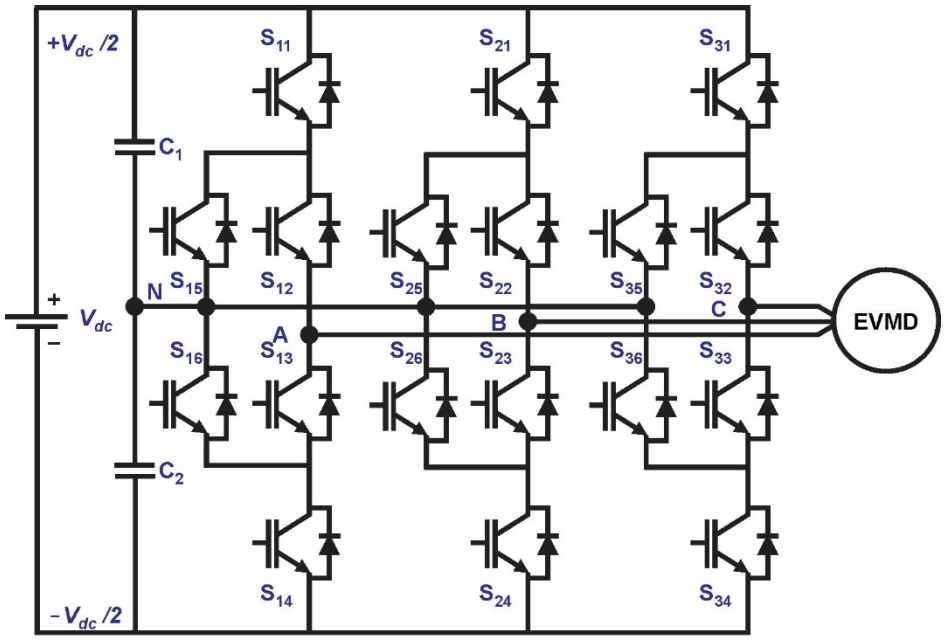

Figure 4. Topology of a 3-phase, 3-level active NPC MLI.

3.3. Flying Capacitor MLI

CHB and NPC technologies were closely followed by the development of a FC low-power topology that is primarily used in medium-voltage FACTS and motor drive applications, especially in traction drives. The FC MLI topology is like the NPC topology, where the clamping diodes are simply replaced by flying capacitors, as can be seen in Figure 5.

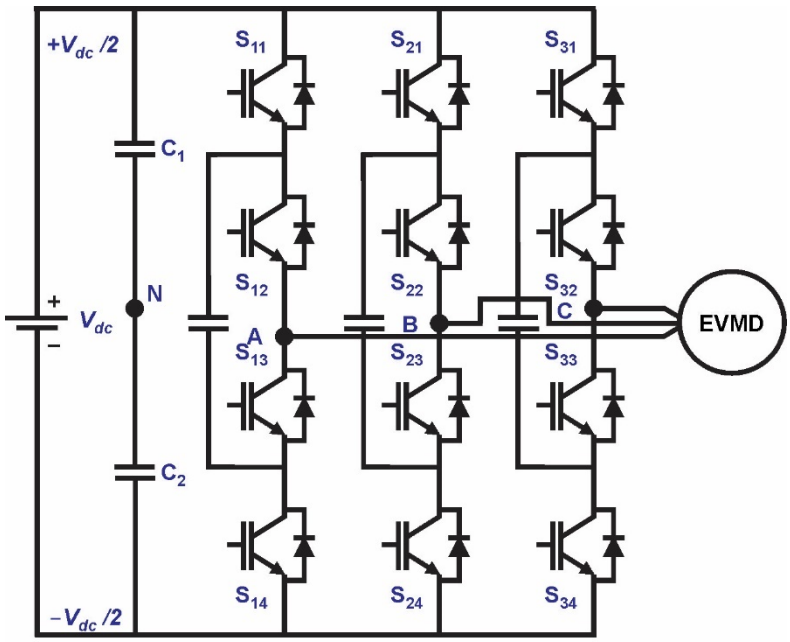

Figure 5. Topology of a 3-phase, 3-level FC MLI.

In this inverter topology, the zero-voltage level cannot be generated directly by connecting the load to the neutral point, but it is achieved by connecting the load through the flying capacitor with DC-link opposite polarity to the positive or negative bar. In FC topology, the four switching states seen in Table 7 are allowed, and two of them generate zero voltage levels. This redundancy can be exploited for power loss optimization.

Table 7. A 3-level FC MLI allows switching states and output voltage levels.

Switching States	S_{11}	S_{12}	S_{13}	S_{14}	Output Voltage
1	1	1	0	0	$V_{dc}/2$
2	1	0	1	0	0
3	0	1	1	0	0
4	0	0	1	1	$-V_{dc}/2$

The main feature of FC topology is its modular structure based on the connection of several simple power cells that consist of two semiconductor power devices and one flying capacitor, where each cell adds one extra level in output voltage. By applying the well-known multicarrier phase-shifted PWM modulation techniques to equalize losses, the excellent quality of the output voltage waveform and the balanced naturally floating DC voltages can be achieved. The main drawbacks are bulky capacitors that are unreliable and increase the complexity of the control circuit and the slow dynamic response of the natural DC voltage balancing, all of which make FC MLI less suitable for BEVs.

3.4. MLIs: Design and Power Loss Considerations

In previous subsections, MLI topologies have now become regarded as classic or traditional MLI configurations that have been successfully implemented as industrial products over the past two decades. Multiple manufacturers in the field have commercialized these inverters, offering varying power ratings, front-end configurations, cooling systems, semiconductor devices, control schemes, and other technical specifications. Among these, the 3-level NPC and CHB MLIs have gained the most popularity in industrial applications.

As already stated, the MLIs offer desirable characteristics for medium- to high-voltage, high-power applications. However, they have more complex topologies than traditional 2-level inverters, and their operation is not straightforward, involving problems to be

solved. From Table 8, where the formulas to calculate the number of components for all three MLI topologies for m-level output voltage generation are given, it can be concluded that all topologies rely on the same number of semiconductor switches. The number of diodes significantly increases with the number of levels (m) in the output voltage in NPC MLI, limiting its industrial usage to 3-level topologies due to the complex mechanical arrangement of non-symmetrical power switches. Similarly, the number of flying capacitors increases in FC MLI topology, and due to their bulkiness, the inverter dimensions also significantly increase, making them less suitable for BEV applications.

Table 8. Component numbers in classical MLI topologies for *m*-level output voltage.

Topology	No. of DC Voltage Sources V_{dc}	No. of Switches	No. of Capacitors	No. of Diodes	Max. and Min. Output Voltages
NPC MLI	1	$2(m-1)$	$(m-1)$	$(m-1)(m-2)$	$+V_{dc}/2$, $-V_{dc}/2$
FC MLI	1	$2(m-1)$	$(m-1)+(m-1)(m-2)/2$	0	$+V_{dc}/2$, $-V_{dc}/2$
CHB MLI	$(m-1)/2$	$2(m-1)$	0	0	$+((m-1)/2)V_{dc}$, $-((m-1)/2)V_{dc}$

Apparently, a higher-level inverter output voltage can be generated by either more separated DC voltage sources or more components. As higher levels in inverter output voltage offer the possibility to enhance operating characteristics, such as power quality, efficiency, and fault-tolerant operation, which are not feasible in classical inverter topologies, a lot of research efforts have been dedicated to finding the MLI topology that allows achieving a higher-level output voltage with as few separated DC voltage sources and components as possible. As a result, many new reduced-component MLI topologies have been recently introduced that can be divided into the following categories: symmetrical MLI (with or without H-bridge), asymmetrical MLI (with or without H-bridge), and hybrid MLI topologies.

In [32], a comprehensive overview of classical and advanced reduced switch MLI topologies, along with different control schemes and their various power system applications, is presented, indicating that many features of the recently developed switch reduced MLI topologies, such as cost effectiveness, reduced volume, and ease of control, make them superior over classical MLI topologies. Unfortunately, the overview does not cover the application of MLI in BEVs, where efficiency and reliability are the most important features. This topic is addressed in [19], where a multilevel cascade inverter has been proposed to be used in variable types of heavy-duty EVs such as BEVs and hybrid electric vehicles (HEVs), and in [33], where a comprehensive review of power electronics technologies in EVs with a focus on inverter topologies for electric traction drives is presented. A comprehensive review focused on reduced-switch MLI for EV applications is discussed in [34]. The comparative analysis of different latest topologies based on component count, efficiency, and THD of the inverter's output voltage shows that the highest working efficiency of 99.4% is achieved with 3-level active NPC MLI and the lowest THD of 1.6% with interleaved 9-level FC MLI in high power applications.

Recently, many authors proposed and analyzed the working principle of reduced-component MLI topologies with voltage boosting capability up to twice the voltage gain originally intended for transformer-less grid-connected PV applications [35–37]. As they exhibit inherent capacitor voltage self-balancing, no additional balancing circuit is needed, resulting in a compact, high-power density structure, which makes them good candidates for low DC-link voltage BEV applications.

In any battery-supplied power system, operation efficiency is of primary concern, so loss analysis is important when deciding on inverter topology. Semiconductor component power losses can be divided into three categories: conduction losses, switching losses, and blocking losses (normally neglected), which can be either analytically calculated for specific MLI topologies or estimated by simulations. As conduction losses appear on semiconductor

components during conduction state, they depend on inverters' operational point correlated current and on state component resistances, so in principle, inverter topologies with fewer semiconductor components operate with fewer conduction losses when the same type of switch is applied. Switching losses are wasted power dissipated during switching on and off the semiconductor switch, occurring also on antiparallel diodes, so they are highly correlated to the switching frequency and depend on the standing voltage of the switches and the adopted modulation strategy. Power loss evaluation in MLI topologies is a highly demanding task, as the current through each power switch can differ, resulting in a different on-state ratio. Additionally, the power switches can work with different switching frequencies. On-line model-based calculation of power losses in 7-level CHB MLI with IGBT switches is presented in [38].

Even though MLI topologies consist of more components than conventional 2-level inverters, their efficiency is higher because they use lower-rated switches with lower on-state resistance, especially when operating at a higher switching frequency.

4. Comparison between MLIs and Conventional 2-Level Inverters

The main challenges in BEV inverters are to obtain a high power density, high efficiency, small size, rugged, low cost, and high reliability topology and electronics for controlling an electric motor [39].

For BEVs, it is very important to operate with high efficiency to utilize the battery energy as much as possible to either increase the driving range or offer the possibility of expensive battery pack minimization. Additionally, lower losses reduce the size of the required cooling system, which positively impacts component packaging in BEVs and overall power system costs. Many studies confirmed that in BEVs with high-speed electric motors or higher power demands, the MLI topology could be beneficial compared to the conventional 2-level voltage source inverter (VSI) topology shown in Figure 1 and the most widely used for EV propulsion systems.

4.1. CHB MLI versus 2-Level Inverter

The efficiency and cost comparison of a 7-level CHB MLI using low-voltage Si MOSFETs and 2-level inverters using IGBTs or SiC (silicon carbide) MOSFETs with 360 V blocking voltage for automotive applications is presented in [40]. Based on the inverter's power and thermal models and their comparison with a reference vehicle model over various driving cycles, it was found that the CHB MLI with Si MOSFETs has a relatively higher efficiency and can be realized with lower cost among the three compared inverter topologies when the worst case of cost and optimization of the battery pack with CHB MLI are considered. All three inverters operate with the highest efficiency in a standard highway driving cycle because of the high speed, with a 2–3% efficiency improvement in CHB MLI compared to a 2-level IGBT inverter. A CHB MLI efficiency improvement of 10% was found during the urban driving cycle. In both driving cycles, the 2-level SiC MOSFET inverter operates with slightly lower efficiency when compared to the CHB MLI. In addition to efficiency and cost, other factors such as weight, volume, reliability, THD, and EMI, the complexity of control, and the overall design of the electric powertrain greatly influence the suitability of CHB MLI for implementation in BEVs, in which CHB MLI shows advantages and disadvantages over conventional 2-level inverters. As CHB MLI consists of more components, it is inevitably heavier and more voluminous with a lower power density, which can be seen as its disadvantage. However, as it generates the output voltage with a lower THD, lower current harmonics are consequently generated in the electric motor, which, according to [41], influences the increased efficiency of the motor drive system, enabling battery optimization. As a result, the weight of the overall power system remains almost the same as with the 2-level inverter. Furthermore, integrating H-bridge modules as basic components of CHB MLI into the battery pack is proposed as an optimal method to overcome vehicle packaging difficulties due to the larger CHB MLI volume.

Another evaluation and comparison of 2-level inverters with IGBTs and CHB MLI with MOSFETs for EVs using modularized battery topology and operating in different standard drive cycles (NEDC, SFTP-US06, HWFET, and FTP75) is presented in [42]. Given results show that CHB MLI with capacitors in parallel at the input improves the drive system efficiency in all operating conditions when compared with a 2-level inverter. At the same time, this is also valid without capacitors except for the SFTP-US06 drive cycle, where more power is demanded due to higher speeds, resulting in higher battery losses for the CHB MLI drive system.

Similarly, in [43], an investigation is presented on the influence of adding filter capacitors at the input of the CHB MLI in an EV application, confirming that lower current stress on the battery and decreased battery losses can be achieved and, therefore, the enhancement of the battery drive cycle efficiency relative to the added weight and cost is feasible. If 4% of additional filter capacitors are placed at the input of CHB MLI, a 10% loss reduction at a 25 °C battery temperature was indicated by the drive cycle analysis. As the battery loss reduction depends on the applied modulation technique, load torque, and speed, it is suggested to investigate the possibility of an online battery impedance spectroscopy implementation as the battery parameters vary due to climate conditions and aging.

CHB MLI operates with multiple isolated DC sources available when the vehicle energy storage system is organized as a modularized battery topology. In this case, CHB MLI enables better battery pack utilization because cells/modules can be selectively discharged instead of using resistors to be passively balanced by discharging over them. Optimization of a CHB MLI in BEVs concerning the number of battery modules is presented in [44]. CHB MLI configuration is also the most efficient cost solution when different manufacturing costs and battery pack sizes are considered due to higher efficiency and lower energy consumption. The four modules per phase are found to be the best compromise between efficiency and cost, and paralleling smaller switches is proposed instead of using fewer, larger switches.

4.2. A 3-Level NPC MLI versus 2-Level Inverter

Nowadays, NPC MLI is applied as a standard topology with one DC voltage source in many applications.

An examination of 2-level inverters and 3-level NPC MLI is presented in [45]. The comparison between inverters was made regarding inverter efficiency, BEV power drive system application efficiency, THD, and fault tolerance. The results show better THD for the 3-level NPC MLI over all operation points. As modern electrical motors operate at increased electrical frequencies, higher switching frequencies become unavoidable, and at switching frequencies above 8 kHz, the 3-level NPC MLI was found superior to the 2-level inverter when considering the cost. The applications of multilevel inverters in BEVs with a 400-V DC link are limited because of the higher cost compared to 2-level inverters. On the other side, in BEVs with 800-V DC link switches with a blocking capability of 1200 V are required in 2-level inverters, therefore increasing the cost considerably and significantly reducing the efficiency of the inverter, while for 3-level NPC MLI, the standard 650 V switches can still be used, making them more comparable in cost or even a more cost-efficient solution.

The comparison with a standard 2-level inverter and NPC MLIs of 3-level, 5-level, and 7-level was made in [46], where it is shown that the best inverter efficiency is achieved when new WBG SiC and GaN power switches are used because they operate with almost negligible switching losses, so the operation of the inverter at very high switching frequencies is possible. When the efficiency of the complete system consisting of the inverter, electric motor, and filter was analyzed, it was found that with a higher number of levels in NPC MLI, the efficiency was increased due to the used switches having a lower voltage blocking capability and requiring smaller filters. Finally, it was confirmed that for the investigated 5.5 kW induction motor and 5-level NPC MLI, the volume and weight of the filter can be reduced by 70% because of the high switching frequency and more levels in

the inverter output voltage. The complete system efficiency was 98.5% at 25 °C and 98.2% at 150 °C junction temperatures, with an improvement of 2.1% at 25 °C and 2.8% at 150 °C when compared to a 2-level IGBT inverter operating with a 5 kHz switching frequency. Furthermore, fewer power losses in the inverter reduce the cooling effort, resulting in the inverter's smaller size.

The potential benefits when NPC MLI is tied to a modular battery bank were analyzed in [47]. A comparison with a conventional 2-level inverter was performed under the selected design scenario for a small power (50 kW) BEV with a 300-V DC link, a medium power (100 kW) BEV with a 600-V DC link, and a high power (150 kW) BEV with a 900-V DC link in several terms: complexity, modularity, battery SoC balancing, inverter loss, ac voltage harmonic distortion of the electric motor, common mode motor voltage, and reliability. For NPC MLI topologies used for different BEVs, the battery bank was configured as a serial connection of one, two, or three standard 300-V battery packs. The 2-level inverter was operated with standard space vector modulation strategy and NPC MLI with virtual vector PWM strategy [48], which can guarantee well-balanced power extract from each 300-V standard battery pack forming DC link, thus maintaining a good SoC balancing of all series connected battery elements to support the extended battery pack life. The presented results of the study confirm the superiority of NPC MLI over 2-level inverters in terms of modularity, battery SoC balancing, and strong potential for reduction of inverter losses, reduction of THD of electric motor voltage, and RMS common-mode voltage, while NPC MLI shows shortcomings regarding inverter complexity requiring an efficient and reliable assembly approach.

4.3. Comparison Results of Different Inverter Topologies

In a similar way to [9], but using an extended set of several important criteria for BEV applications, comparison results between conventional 2-level inverters, 3-level NPC, and CHB MLIs are summarized in Figure 6, indicating that lower THD, lower voltage stress, fault tolerance, and reliability are the main strengths of CHB and NPC MLI topologies, while lower control complexity is the main strength of conventional 2-level inverters.

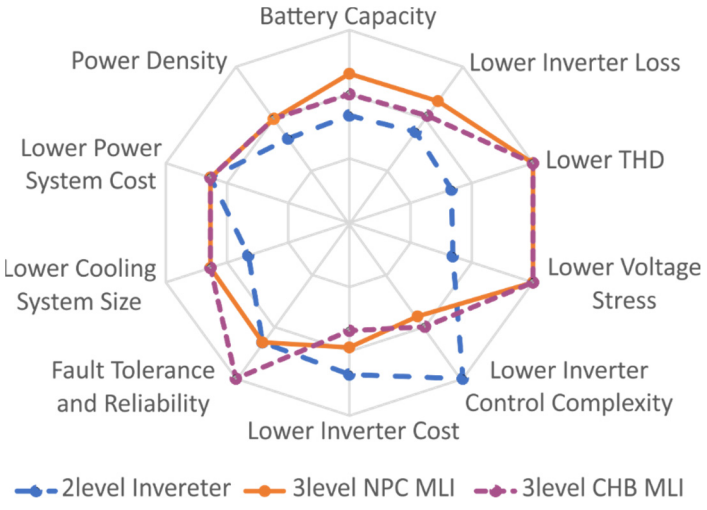

Figure 6. Comparison of different criteria between 2-level inverters, 3-level NPCs, and CHB MLIs.

5. State-of-the-Art of MLIs in All Electric Vehicles

MLI presents an appealing solution for various applications due to its numerous advantages, including high efficiency and power quality. One of its key strengths is the utilization of low-rate power devices, such as GaN and SiC, which are innovative WBG devices. In contrast, conventional 2-level inverters encounter challenges like high dv/dt, high blocking voltage across power devices, and common mode voltage issues. These difficulties can lead to overheating problems and even failures in electric motor windings.

In comparison, MLI generates an output voltage with a sinusoidal-like shape, resulting in reduced THD and dv/dt. As a result, power devices and electric motors experience lower levels of stress. MLI also enables the handling of high power at low switching frequencies, leading to reduced switching losses. Moreover, it operates with a low common voltage, which further decreases the strain on electric motor bearings and extends their lifespan. Overall, these advantages contribute to the enhanced performance and durability of MLI-based systems.

5.1. MLI in Electric Railway

As already said, the advantage of using low-rated power devices in MLIs made them more suitable for high-power and medium-voltage (between 1 and 35 kV according to the International Standard of the International Electrotechnical Commission) applications. In 1988, a 3-level NPC GTO-based MLI was first proposed to efficiently substitute a conventional 2-level inverter for an induction motor in locomotives [49], and Siemens AD successfully tested the proposed topology in the TRANSRAPID propulsion system. In [49], a proposal is made to use a 7-level CHB MLI as a STATCOM (Static Synchronous Compensator) to provide reactive power compensation for the railway system and regulate its voltage. The application involves several aspects, including determining the necessary reactive power for the railway system, designing the multilevel inverter STATCOM to meet the requirements of the railway grid, developing a control system to regulate the system's voltage, and evaluating the performance of the STATCOM-compensated railway system under steady-state and transient conditions.

The MLI-based propulsion system for railway transportation electrification, where high-efficiency voltage regulation at all load conditions is achieved by space vector PWM and additional back-to-back clamped diode voltage modulation, is presented in [50]. Zero-current switching combined with control algorithms that eliminate the unwanted harmonics from the output voltage result in an increased operating efficiency of 98.5% at full load for a 1000-Vdc/700-Vac 400 kW inverter compared with the previous efficiency of 97%. The proposed inverter topology also provides better cost efficiency when compared to conventional hard-switched 2-level PWM-controlled inverters.

5.2. MLI in Electric Ships

In all-electric ships, medium-voltage DC systems are recognized as the next generation of ship-integrated power systems since they offer significant operational and economic merits [51], where the medium-voltage inverter for the electric motor plays the role of one of the most powerful components due to the improved energy conversion efficiency and fault-tolerant ability. Due to specific requirements of electric ship applications such as space constraints and self-generating power systems, high power quality, power density, reliability, lower insulation stress, and fault tolerance are the most important features [52]. The modular MLI was proposed as the most suitable topology for complying with the shipboard requirements. A family of symmetrical hybrid MLI for a five-phase induction motor-based propulsion system is presented in [53], where each phase in the inverter topology consists of a multilevel DC/DC converter operating at high frequency and an H-bridge cell operating at fundamental frequency. The obtained results of the neutral point voltage balancing method based on a modified phase-shifted PWM modulation strategy confirmed the effectiveness of the proposed system. A unique hierarchical redundancy design of modular MLI that can assure uninterrupted operation of an electric ship medium-voltage DC system is proposed in [54].

5.3. MLI in Aircraft

Higher energy efficiencies, lower greenhouse emissions, and lower audible noise have become critical issues for more sustainable aviation. As aviation is considered the most rapidly growing industry in the transportation sector, the electrification of aircraft is seen as the best possibility to reduce the environmental effects of aviation [55]. In all-electric

aircraft, all power systems are powered by electrical sources, including propulsion systems with large-scale power converters. In [56], a 9-level CHB MLI is proposed as a suitable solution to feed the 3-phase permanent magnet synchronous motor in all-electric aircraft. Experimental validation confirmed increased efficiency of the propulsion system, lower THD, and reduced motor torque ripple. Applying a 3-level active neutral point clamped (ANPC) MLI with the combination of WBG SiC MOSFETs and silicon IGBT switches for a high-MW power-scale motor drive is suggested in [57]. For the same inverter topology, the new PWM modulation strategy assuring soft switching across all IGBTs and small loss dissipation only on SiC MOSFETs is proposed in [58], resulting in inverter operation with efficiency as high as 99% for the 1.2 MVA/1 MW application case.

5.4. MLI in Road Transport

Recently, MLIs have been the subject of many studies in low-voltage hybrid or all-electric heavy-duty (trucks, buses) and passenger EVs [19,34,45,59–64].

Back-to-back diode clamped MLI applications were proposed for heavy-duty large hybrid EV trucks and military vehicles, while 11-level CHB MLI was proposed for all-electric vehicles with many available separate DC sources from batteries [19]. Experimental verification confirmed that MLI inverters can operate more efficiently than 2-level conventional PWM inverters. At load conditions, greater than 40% of the rated power MLI was operated with 98% efficiency, while the 2-level PWM inverter achieved the highest efficiency of 95.6% at 90% nominal loads. At small loads, MLI showed even higher superiority considering efficiency. In addition to the well-known advantages of MLI, the authors experimentally confirmed that there are no unbalanced problems during the charging process or drive mode.

Asymmetrical CHB MLI that uses different-sized H-bridges and requires a less isolated DC source than symmetrical CHB was analyzed for application in small EVs [59]. A proposed solution consists of the main H-bridge working at the fundamental frequency and additional small H-bridges operating as series active power filters. By proper design of an asymmetrical CHB and adopting switching strategies, the THD of the output voltage is only 3.5% for the case of 23 levels.

A CHB multilevel boost inverter implemented without inductors in all hybrid EVs is presented in [64]. The proposed inverter topology consists of a conventional 3-phase 2-level inverter and, in series, an H-bridge connected to each inverter phase with a capacitor used as a DC power supply. A fundamental switching scheme obtains the five-level output voltage. Due to the absence of an inductor, high power density is achieved.

An integration of a 5-level T-Type MLI with a bidirectional DC-DC multilevel converter for EV applications is presented in [60]. The main advantage of the proposed topology is the high-frequency cycle-by-cycle voltage balance between DC bus capacitors, resulting in reduced required capacitance, allowing the use of more reliable, longer-life film capacitors instead of electrolytic capacitors. Consequently, the volume and weight of the inverter could be reduced by 20%, allowing more space for the EV battery pack.

Although numerous studies have been conducted on MLIs for EVs, a conventional 2-level inverter is still used in almost all commercial EV drive systems. However, due to the transition to the high 800-V DC link in EV, it is foreseen that MLIs, with their distinctive advantages, will soon find the path to commercial EV products.

5.5. MLIs on the Market and Future Trends

Although numerous original equipment manufacturers (OEM), suppliers, and researchers in national laboratories are working together to improve the power electronics systems concerning power density and cost, and many studies have been performed on investigating multilevel inverters in different traction applications, the market has not relied on these structures yet, especially in low-power applications.

Recently, the U.S. Department of Energy (DOE), aiming to accelerate EV integration into the market, updated its objectives by defining new targets for inverter power density

and cost to be met by 2025. For the high-voltage 100 kW peak power inverter module integrated design, a power density of 100 kW/L and a cost of $2.7/kW are expected, which represents an 87% volume reduction and an 18% cost reduction compared to the previous set of target goals to be met by 2020. Similarly, the targets for electric traction motors have also been changed to $3.3/kW for the cost and 50 kW/l for the power density, which implies a 30% cost reduction and an 89% volume reduction, respectively.

Table 9 illustrates the configurations of traction inverters, the types of switching devices employed, and the DC voltage levels utilized in various traction applications as given in [9]. Multilevel inverter structures have already been implemented in applications requiring higher power and DC input voltage, such as electric ships, trains, and tramways. Notably, General Electric, ABB, and Siemens have developed multilevel inverters specifically for electric ship applications. Additionally, ABB offers 3-level IGBT inverters, which are characterized by reduced motor stresses and high efficiency, for Swedish State Railways, Swiss Federal Railways, and Deutsche Bahn.

Table 9. Traction inverter structure, DC voltage levels, and switching devices used for different traction applications [9].

Application	Inverter Structure	DC Voltage (V)	Switching Devices
Electric ships	2-level or Multilevel	1.5 kV to 15 kV	GTO, Thyristor, or IGBT
Trains and tramways	2-level or 3-level	Up to 3 kV	GTO, Thyristor, or IGBT
Buses and trucks	2-level or 3-level	Up to 900-V	IGBT or MOSFET
Passenger BEVs	2-level or 3-level	Up to 900-V	IGBT, MOSFET, SiC, or GaN

At present, passengers' BEVs equipped with 400 V batteries predominantly employ 2-level inverters. An extensive examination of inverter structures in popular BEV models can be found in [65], revealing that Tesla and Nissan utilize either six or three parallel switches in their 2-level inverters. This configuration choice is influenced by the low DC-link voltage and high currents associated with these vehicles.

The increasing trend of elevating battery voltage to 800 V in BEVs has opened new possibilities for inverter structures. In 2019, at CTI Berlin, Dana TM4 introduced a groundbreaking silicon carbide (SiC) inverter designed for e-racing. This innovative inverter boasts a remarkable operating voltage range of 450–900 V and exhibits an impressive power density of 195 kW/L. The introduction of SiC power electronics has paved the way for highly efficient inverters and chargers tailored for next-generation battery packs, specifically those operating at 800 V. Recognizing this, several manufacturers, such as Eaton, Marelli, and Denso, have already developed a new series of high-voltage 2-level SiC inverters to cater to automotive plug-in hybrid (PHEV) and BEV applications. These advancements in SiC technology represent a significant direction for future development in the automotive industry.

In past years, German powertrain expert Hofer powertrain has developed an IGBT-based 3-level NPC inverter as part of a 3-in-1 system with an induction motor and a gearbox [66]. Based on this electric drive system, the different effects were investigated in detail. Especially the improvement in electric motor efficiency is of high interest to the automotive industry since this results in less cooling demand and increased performance as well as driving range. The investigations for a 170-kW induction motor conducted by a Hofer powertrain show that electric motor losses in the Worldwide Harmonized Light Vehicles Test Procedure (WLTP) drive cycle can be reduced by 25%. Any other measure for efficiency improvement cannot achieve such an outstanding improvement.

Additionally, when looking at NVH characteristics, measurements on the electric motor side showed that noise can also be reduced by about 25% due to the better THD of the output current. In the same magnitude, improvements in EMC behavior were observed.

These effects can either be used to reach a higher level of requirements for the electric drive or can be considered a degree of freedom to reduce efforts within the EMC filter of the inverter, NVH damping of the electric drive train, or countermeasures on bearing currents.

This improvement comes at the cost of additional effort on the inverter. Due to the multilevel topology, additional switches have become necessary. Hofer powertrain chose the 3-level NPC inverter topology to reduce the breakdown voltage requirement for the power switches from 1200 V down to 650 V at a battery voltage of up to 950 V. Other additional efforts need to be considered for the DC link capacitor and the gate drive board. Overall, this could result in a minimal increase in inverter volume and more power switches in the power path if careful selection of these power switches is assured. Nowadays, automotive IGBT power modules with a breakdown voltage of 650 V provide a good power-to-cost ratio but show rather poor efficiency from an automotive point of view, especially when combined in a 3-level inverter. In the end, a reduction in the efficiency improvement gained by the electric motor on the electric drive system level can be observed.

Another choice for 3-level inverters is a SiC-based power switch or a hybrid solution out of IGBT and SiC switches and diodes. For such a configuration, the inverter's efficiency should be comparable to that of a conventional 2-level inverter based on SiC power switches for the WLTP drive cycle. The main drawback of a SiC configuration is the high cost of the power switches, regardless of the topology.

In the pursuit of finding the optimal solution, Hofer powertrain, in collaboration with VisIC Technologies, has investigated the use of WBG GaN power switches for a 3-level inverter. WBG GaN power devices have demonstrated promising potential for achieving high-efficiency power conversion. The unique structure of WBG GaN semiconductors enables devices with exceptional transport characteristics and charge density in the channel, allowing them to operate at high voltages. These characteristics facilitate their utilization at higher frequencies with fewer parasitic effects, thus enabling the development of high-power density and high-efficiency inverters [67,68]. This inherent flexibility in device design ensures robust operation and high performance. There are two types of lateral GaN power devices: depletion mode (D-mode) devices, also known as normally on devices, and enhancement mode (E-mode) devices, also known as normally off devices, each with their own advantages and disadvantages. The gate region differs for these two implementations and significantly influences potential reliability. It is crucial to understand these trade-offs in order to make an appropriate choice for a specific application.

VisIC Technologies' D3GaN technology (Direct Drive D-Mode) has been developed to meet the high reliability standards of the automotive industry and offers the lowest losses per RDS (on). The evaluation results of a 650 V, 100 A D3GaN power switch in a top-cooled surface-mount device package in terms of static and dynamic performance, surge energy, and short-circuit robustness are presented in [69]. In comparison with similar voltage and current ratings for GaN HEMT (high-electron-mobility transistor) and SiC MOSFET power switches, the D3 GaN power switch exhibits a higher gate threshold voltage, a smaller total gate charge, a lower device capacitance, and a faster switching speed. As a result, D3GaN technology simplifies the system and enables highly efficient and cost-effective powertrain platform solutions. By reducing the cooling system requirements and inverter size in electric vehicles (EVs), this solution can save up to 50% of inverter power losses over the driving cycle, leading to reduced battery costs and increased driving range. The ability to support vehicles with both 800-V and 400-V batteries marks a significant milestone in the global adoption of GaN technology in automotive electrical drivelines.

The capability to parallel GaN devices is crucial for inverter applications, and the D3GaN topology has been specifically designed to support device paralleling. With direct access to the GaN gates, positive temperature coefficients, and the highest current rating per die (i.e., 200 Amp), this solution facilitates the simplest implementation of GaN systems that meet the high-power demands of the automotive market.

For 800-V applications, critical system development involves utilizing proven 650-V-rated devices in a 3-level inverter. This design demonstrates the ability of GaN devices to enhance 800-V electric motor systems by reducing phase current ripple and improving drive cycle efficiency. Compared to the standard 2-level approach, the D3GaN power switches offer lower total losses, resulting in improved utilization performance. The system is currently undergoing a series of tests in real-world conditions, and it is expected to exceed expectations, ultimately leading to a more efficient vehicle engine.

A comprehensive analysis of the opportunities and challenges for future battery electric vehicles (BEVs), as defined by DOE in their new targets for inverter power density and cost by 2025, is presented in [70]. Increased integration of the inverter within the electric drive system will lead to further enhancements in power density and thermal management, leading to reduced materials used in manufacturing and lower production costs. WBG switches are essential elements for the next generation of inverters, as they can operate at higher frequencies with lower losses, increasing overall inverter efficiency and enabling size reduction by downsizing bulky capacitors. One significant advantage of high-frequency operation is the opportunity to utilize electric motors that can operate at higher speeds, resulting in a smaller overall motor size and substantial cost and packaging savings. Although 3-level inverters are already available on the market, determining the optimal number of levels in a multilevel topology, considering factors, such as inverter complexity, reliability, and control demands, is an ongoing process.

6. Conclusions

The future of the EV market and, closely related to it, the long-term sustainability of our transportation systems depend on advances and improvements in technology, and the development of components such as the inverter plays a fundamental role in making EVs more efficient, affordable, and attractive to the consumer. Many car producers have already moved to high 800-V DC link voltage, especially in an upper class of passengers' BEVs, as this transition supports additional benefits of lighter cables, more efficient electric motors, and higher switching frequency when WBG switches in EV power systems are used, all of which enable power density and inverter cost targets set by the US DoE to be met.

However, higher voltage stress on power semiconductors and increased electromagnetic interference in power systems are two main drawbacks of the increased voltage standard in light-duty passenger BEVs. MLI, with reduced stress on semiconductor switches and reduced electromagnetic interference, high efficiency, intrinsic fault tolerance, and cost competitiveness when considering the entire power system, can be an effective and feasible substitute for conventional 2-level inverters.

A comparison of two classical topologies of MLIs, namely NPC and CHB, versus conventional 2-level inverters according to THD, efficiency, and cost, as well as the usage of different MLI topologies in different transportation modes that have been conducted in this survey, confirm that WBG devices based on 3-level NPC MLI and 5-level CHB MLI as isolated DC sources that can be provided from the batteries, are both good candidates to be used in future high-power passenger BEVs as well as in other EVs. On the other hand, MLI topologies with a high number of flying capacitors (FC MLI) are inadequate for BEV applications since the capacitors are bulky, unreliable, and increase the complexity of the control circuit.

Author Contributions: Conceptualization, A.H. and M.T.; methodology, A.H.; validation, A.H., F.M. and M.T.; formal analysis, A.H., F.M. and M.T.; investigation, A.H.; resources, A.H.; data curation, A.H. and F.M., writing—original draft preparation, A.H.; writing—review and editing, A.H., F.M. and M.T.; funding acquisition, M.T. All authors have read and agreed to the published version of the manuscript.

Funding: Research was funded by the Slovenian Research Agency (ARRS) (Research Core Funding No. P2-0028).

Data Availability Statement: Not applicable.

Conflicts of Interest: The authors declare no conflict of interest.

Abbreviations

The following abbreviations are commonly used in this manuscript:

BEV	Battery electric vehicle
BESS	Battery energy storage system
CHB	Cascade H-bridge
DCC	Diode-clamped converter
HEV	Hybrid electric vehicle
EV	Electric vehicle
FC	Flying capacitor
FACTS	Flexible AC transmission system
GaN	Gallium nitride
ICEV	Internal combustion engine vehicle
MLI	Multilevel inverter
NPC	Neutral point clamped
NVH	Noise, vibration, and harshness
PWM	Pulse-width modulation
RES	Renewable energy sources
SES	Stationary energy storage
SoC	State of charge
THD	Total harmonic distortion
XFC	Extremely fast charging
WBG	Wide bandgap

References

1. Cars, Planes, Trains: Where Do CO_2 Emissions from Transport Come from? Available online: https://ourworldindata.org/co2-emissions-from-transport (accessed on 23 March 2023).
2. Sustainable and Smart Mobility Strategy. Available online: https://ec.europa.eu/info/law/better-regulation/have-your-say/initiatives/12438-sustainable-and-smart-mobility-strategy_en (accessed on 4 April 2023).
3. Adib, A.; Shadmand, M.B.; Shamsi, P.; Afridi, K.K.; Amirabadi, M.; Fateh, F.; Ferdowsi, M.; Lehman, B.; Lewis, L.H.; Mirafzal, B.; et al. E-Mobility—Advancements and Challenges. *IEEE Access* **2019**, *7*, 165226–165240. [CrossRef]
4. Meintz, A.; Zhang, J.; Vijayagopal, R.; Kreutzer, C.; Ahmed, S.; Bloom, I.; Burnham, A.; Carlson, R.B.; Dias, F.; Dufek, E.J.; et al. Enabling Fast Charging—Vehicle Considerations. *J. Power Source* **2017**, *367*, 216–227. [CrossRef]
5. Tu, H.; Feng, H.; Srdic, S.; Lukic, S. Extreme Fast Charging of Electric Vehicles: A Technology Overview. *IEEE Trans. Transp. Electrif.* **2019**, *5*, 861–878. [CrossRef]
6. Deb, N.; Singh, R.; Brooks, R.R.; Bai, K.; Barrero, F.; Kao, M.H. A Review of Extremely Fast Charging Stations for Electric Vehicles. *Energies* **2021**, *14*, 7566. [CrossRef]
7. Electric Vehicle Database. Available online: https://ev-database.org/ (accessed on 25 May 2023).
8. Bubert, A.; Oberdieck, K.; Xu, H.; De Doncker, R.W. Experimental Validation of Design Concepts for Future EV-Traction Inverters. In Proceedings of the 2018 IEEE Transportation and Electrification Conference and Expo, ITEC 2018, Long Beach, CA, USA, 13–15 June 2018; Institute of Electrical and Electronics Engineers Inc.: Piscataway, NJ, USA, 2018; pp. 347–352.
9. Poorfakhraei, A.; Narimani, M.; Emadi, A. A Review of Multilevel Inverter Topologies in Electric Vehicles: Current Status and Future Trends. *IEEE Open J. Power Electron.* **2021**, *2*, 155–170. [CrossRef]
10. Jung, C. Power Up with 800-V Systems: The Benefits of Upgrading Voltage Power for Battery-Electric Passenger Vehicles. *IEEE Electrif. Mag.* **2017**, *5*, 53–58. [CrossRef]
11. Keyser, M.; Pesaran, A.; Li, Q.; Santhanagopalan, S.; Smith, K.; Wood, E.; Ahmed, S.; Bloom, I.; Dufek, E.; Shirk, M.; et al. Enabling Fast Charging—Battery Thermal Considerations. *J. Power Source* **2017**, *367*, 228–236. [CrossRef]
12. Burnham, A.; Dufek, E.J.; Stephens, T.; Francfort, J.; Michelbacher, C.; Carlson, R.B.; Zhang, J.; Vijayagopal, R.; Dias, F.; Mohanpurkar, M.; et al. Enabling Fast Charging—Infrastructure and Economic Considerations. *J. Power Source* **2017**, *367*, 237–249. [CrossRef]
13. Rafi, M.A.H.; Bauman, J. A Comprehensive Review of DC Fast-Charging Stations with Energy Storage: Architectures, Power Converters, and Analysis. *IEEE Trans. Transp. Electrif.* **2021**, *7*, 345–368. [CrossRef]
14. Islam, R.; Rafin, S.M.S.H.; Mohammed, O.A. Comprehensive Review of Power Electronic Converters in Electric Vehicle Applications. *Forecasting* **2022**, *5*, 2. [CrossRef]

15. Powar, V.; Singh, R. End-to-End Direct-Current-Based Extreme Fast Electric Vehicle Charging Infrastructure Using Lithium-Ion Battery Storage. *Batteries* **2023**, *9*, 169. [CrossRef]
16. Copper Drives Electric Vehicles. Available online: https://www.copper.org/publications/pub_list/pdf/a6191-electricvehicles-factsheet.pdf (accessed on 4 April 2023).
17. Leon, J.I.; Vazquez, S.; Franquelo, L.G. Multilevel Converters: Control and Modulation Techniques for Their Operation and Industrial Applications. *Proc. IEEE* **2017**, *105*, 2066–2081. [CrossRef]
18. Alavi, O.; Viki, A.H.; Shamlou, S. A Comparative Reliability Study of Three Fundamental Multilevel Inverters Using Two Different Approaches. *Electronics* **2016**, *5*, 18. [CrossRef]
19. Tolbert, L.M.; Peng, F.Z.; Habetler, T.G. Multilevel Inverters for Electric Vehicle Applications. In Proceedings of the IEEE Workshop on Power Electronics in Transportation, WPET 1998, Dearborn, MI, USA, 22–23 October 1998; IEEE: Piscataway, NJ, USA, 1998.
20. Rodríguez, J.; Lai, J.S.; Peng, F.Z. Multilevel Inverters: A Survey of Topologies, Controls, and Applications. *IEEE Trans. Ind. Electron.* **2002**, *49*, 724–738. [CrossRef]
21. Rodriguez, J.; Bernet, S.; Steimer, P.K.; Lizama, I.E. A Survey on Neutral-Point-Clamped Inverters. *IEEE Trans. Ind. Electron.* **2010**, *57*, 2219–2230. [CrossRef]
22. Nabae, A.; Takahashi, I.; Akagi, H. A New Neutral-Point-Clamped PWM Inverter. *IEEE Trans. Ind. Appl.* **1981**, *IA-17*, 518–523. [CrossRef]
23. Matsui, K.; Kawata, Y.; Ueda, F. Application of Parallel Connected NPC-PWM Inverters with Multilevel Modulation for AC Motor Drive. *IEEE Trans. Power Electron.* **2000**, *15*, 901–907. [CrossRef]
24. Enjeti, P.N.; Jakkli, R. Optimal Power Control Strategies for Neutral Point Clamped (NPC) Inverter Topology. *IEEE Trans. Ind. Appl.* **1992**, *28*, 558–566. [CrossRef]
25. Sebaaly, F.; Vahedi, H.; Kanaan, H.Y.; Moubayed, N.; Al-Haddad, K. Design and Implementation of Space Vector Modulation-Based Sliding Mode Control for Grid-Connected 3L-NPC Inverter. *IEEE Trans. Ind. Electron.* **2016**, *63*, 7854–7863. [CrossRef]
26. Wang, Y.; Li, R. Novel High-Efficiency Three-Level Stacked-Neutral-Point-Clamped Grid-Tied Inverter. *IEEE Trans. Ind. Electron.* **2013**, *60*, 3766–3774. [CrossRef]
27. Brückner, T.; Bernet, S.; Güldner, H. The Active NPC Converter and Its Loss-Balancing Control. *IEEE Trans. Ind. Electron.* **2005**, *52*, 855–868. [CrossRef]
28. Zhang, L.; Zheng, Z.; Li, C.; Ju, P.; Wu, F.; Gu, Y.; Chen, G. A Si/SiC Hybrid Five-Level Active NPC Inverter with Improved Modulation Scheme. *IEEE Trans. Power Electron.* **2020**, *35*, 4835–4846. [CrossRef]
29. Li, J.; Huang, A.Q.; Liang, Z.; Bhattacharya, S. Analysis and Design of Active NPC (ANPC) Inverters for Fault-Tolerant Operation of High-Power Electrical Drives. *IEEE Trans. Power Electron.* **2012**, *27*, 519–533. [CrossRef]
30. Ma, L.; Kerekes, T.; Rodriguez, P.; Jin, X.; Teodorescu, R.; Liserre, M. A New PWM Strategy for Grid-Connected Half-Bridge Active NPC Converters with Losses Distribution Balancing Mechanism. *IEEE Trans. Power Electron.* **2015**, *30*, 5331–5340. [CrossRef]
31. Guan, Q.X.; Li, C.; Zhang, Y.; Wang, S.; Xu, D.D.; Li, W.; Ma, H. An Extremely High Efficient Three-Level Active Neutral-Point-Clamped Converter Comprising SiC and Si Hybrid Power Stages. *IEEE Trans. Power Electron.* **2018**, *33*, 8341–8352. [CrossRef]
32. Choudhury, S.; Bajaj, M.; Dash, T.; Kamel, S.; Jurado, F. Multilevel Inverter: A Survey on Classical and Advanced Topologies, Control Schemes, Applications to Power System and Future Prospects. *Energies* **2021**, *14*, 5773. [CrossRef]
33. Sayed, K.; Almutairi, A.; Albagami, N.; Alrumayh, O.; Abo-Khalil, A.G.; Saleeb, H. A Review of DC-AC Converters for Electric Vehicle Applications. *Energies* **2022**, *15*, 1241. [CrossRef]
34. Aishwarya, V.; Gnana Sheela, K. Review of Reduced-Switch Multilevel Inverters for Electric Vehicle Applications. *Int. J. Circuit Theory Appl.* **2021**, *49*, 3053–3110. [CrossRef]
35. Chen, M.; Yang, Y.; Liu, X.; Loh, P.C.; Blaabjerg, F. Single-Source Cascaded Multilevel Inverter with Voltage-Boost Submodule and Continuous Input Current for Photovoltaic Applications. *IEEE Trans. Power Electron.* **2022**, *37*, 955–970. [CrossRef]
36. Siddique, M.D.; Aslam Husain, M.; Iqbal, A.; Mekhilef, S.; Riyaz, A. Single-Phase 9L Switched-Capacitor Boost Multilevel Inverter (9L-SC-BMLI) Topology. *IEEE Trans. Ind. Appl.* **2023**, *59*, 994–1001. [CrossRef]
37. Lee, S.S.; Bak, Y.; Kim, S.M.; Joseph, A.; Lee, K.B. New Family of Boost Switched-Capacitor Seven-Level Inverters (BSC7LI). *IEEE Trans. Power Electron.* **2019**, *34*, 10471–10479. [CrossRef]
38. Alamri, B.; Darwich, M. Precise Modelling of Switching and Conduction Losses in Cascaded H-Bridge Multilevel Inverters. In Proceedings of the 49th International Universities Power Engineering Conference (UPEC), Cluj-Napoca, Romania, 2–5 September 2014.
39. Rajashekara, K. Present Status and Future Trends in Electric Vehicle Propulsion Technologies. *IEEE J. Emerg. Sel. Top. Power Electron.* **2013**, *1*, 3–10. [CrossRef]
40. Chang, F.; Ilina, O.; Lienkamp, M.; Voss, L. Improving the Overall Efficiency of Automotive Inverters Using a Multilevel Converter Composed of Low Voltage Si Mosfets. *IEEE Trans. Power Electron.* **2019**, *34*, 3586–3602. [CrossRef]
41. Li, H.; Klontz, K.W. An Investigation of Current Harmonic Influence on Induction Motor in Hybrid Electric Vehicle Application. In Proceedings of the 2017 IEEE International Electric Machines and Drives Conference, IEMDC 2017, IEEE, Miami, FL, USA, 21–24 May 2017.

42. Josefsson, O.; Thiringer, T.; Lundmark, S.; Zelaya, H. Evaluation and Comparison of a Two-Level and a Multilevel Inverter for an EV Using a Modulized Battery Topology. In Proceedings of the IEEE Industrial Electronics Conference IECON 2012, Montreal, QC, Canada, 25–28 October 2012.
43. Kersten, A.; Theliander, O.; Grunditz, E.A.; Thiringer, T.; Bongiorno, M. Battery Loss and Stress Mitigation in a Cascaded H-Bridge Multilevel Inverter for Vehicle Traction Applications by Filter Capacitors. *IEEE Trans. Transp. Electrif.* **2019**, *5*, 659–671. [CrossRef]
44. Roemer, F.; Ahmad, M.; Chang, F.; Lienkamp, M. Optimization of a Cascaded H-Bridge Inverter for Electric Vehicle Applications Including Cost Consideration. *Energies* **2019**, *12*, 4272. [CrossRef]
45. Bubert, A.; Lim, S.-H.; De Doncker, R.W. Comparison of 2-Level B6C and 3-Level NPC Inverter Topologies for Electric Vehicles. In Proceedings of the 2017 IEEE Southern Power Electronics Conference, PESC, Puerto Varas, Chile, 4–7 December 2017.
46. Mecke, R. Multilevel Inverter with New Wide-Bandgap SiC and GaN Power Switches. In Proceedings of the 2021 IEEE 15th International Conference on Compatibility, Power Electronics and Power Engineering, CPE-POWERENG 2021, Florence, Italy, 14–16 July 2021.
47. Busquets-Monge, S.; Alepuz, S.; García-Rojas, G.; Bordonau, J. Electric Vehicle Powertrains with Modular Battery Banks Tied to Multilevel NPC Inverters. *Electronics* **2023**, *12*, 266. [CrossRef]
48. Busquets-Monge, S. A Simple Virtual-Vector-Based PWM Formulation for Multilevel Three-Phase Neutral-Point-Clamped DC–AC Converters Including the Overmodulation Region. *Electronics* **2022**, *11*, 641. [CrossRef]
49. Steinke, J.K. ontrol Strategy for a Three Phase AC Traction Drive with Three-Level GTO PWM Inverter. In Proceedings of the PESC Record—IEEE Annual Power Electronics Specialists Conference PESC 1988, Kyoto, Japan, 11–14 April 1988.
50. Youssef, M.Z.; Woronowicz, K.; Aditya, K.; Azeez, N.A.; Williamson, S.S. Design and Development of an Efficient Multilevel DC/AC Traction Inverter for Railway Transportation Electrification. *IEEE Trans. Power Electron.* **2016**, *31*, 3036–3042. [CrossRef]
51. Yang, G.; Xiao, F.; Fan, X.; Wang, R.; Liu, J. Three-Phase Three-Level Phase-Shifted PWM DC-DC Converter for Electric Ship MVDC Application. *IEEE J. Emerg. Sel. Top. Power Electron.* **2017**, *5*, 162–170. [CrossRef]
52. Ronanki, D.; Williamson, S.S. Modular Multilevel Converters for Transportation Electrification: Challenges and Opportunities. *IEEE Trans. Transp. Electrif.* **2018**, *4*, 399–407. [CrossRef]
53. Wenfeng, L.; Nianzhou, L.; Kui, W.; Zedong, Z.; Yongdong, L. Symmetrical Hybrid Multilevel Inverters for Ship Electric Propulsion Drives. In Proceedings of the IEEE 4th International Future Energy Electronics Conference (IFEEC), Singapore, 24–28 November 2019.
54. Chen, Y.; Li, Z.; Zhao, S.; Wei, X.; Kang, Y. Design and Implementation of a Modular Multilevel Converter with Hierarchical Redundancy Ability for Electric Ship MVDC System. *IEEE J. Emerg. Sel. Top. Power Electron.* **2017**, *5*, 189–202. [CrossRef]
55. Schefer, H.; Fauth, L.; Kopp, T.H.; Mallwitz, R.; Friebe, J.; Kurrat, M. Discussion on Electric Power Supply Systems for All Electric Aircraft. *IEEE Access* **2020**, *8*, 84188–84216. [CrossRef]
56. Patel, V.; Buccella, C.; Cecati, C. Analysis and Implementation of Multilevel Inverter for Full Electric Aircraft Drives. *Energies* **2020**, *13*, 6126. [CrossRef]
57. Zhang, D.; He, J.; Pan, D. A Megawatt-Scale Medium-Voltage High-Efficiency High Power Density "SiC+Si" Hybrid Three-Level ANPC Inverter for Aircraft Hybrid-Electric Propulsion Systems. *IEEE Trans. Ind. Appl.* **2019**, *55*, 5971–5980. [CrossRef]
58. He, J.; Zhang, D.; Pan, D. PWM Strategy for MW-Scale "SiC+Si" ANPC Converter in Aircraft Propulsion Applications. *IEEE Trans. Ind. Appl.* **2021**, *57*, 3077–3086. [CrossRef]
59. Pereda, J.; Dixon, J. 23-Level Inverter for Electric Vehicles Using a Single Battery Pack and Series Active Filters. *IEEE Trans. Veh. Technol.* **2012**, *61*, 1043–1051. [CrossRef]
60. Sheir, A.; Youssef, M.Z.; Orabi, M. A Novel Bidirectional T-Type Multilevel Inverter for Electric Vehicle Applications. *IEEE Trans. Power Electron.* **2019**, *34*, 6648–6658. [CrossRef]
61. Li, Z.; Khajepour, A.; Song, J. A Comprehensive Review of the Key Technologies for Pure Electric Vehicles. *Energy* **2019**, *182*, 824–839. [CrossRef]
62. Roy, P.; Banerjee, A. A Study on Performance Parameters of Three-Level T-Type Inverter Based PMSM Drives for Electric Vehicles Applications. *Electr. Eng.* **2023**, 105. [CrossRef]
63. Josefsson, O. Investigation of a Multilevel Inverter for Electric Vehicle Applications. Doctoral Thesis, Chalmers University of Technology, Göteborg, Sweden, 2015.
64. Du, Z.; Ozpineci, B.; Tolbert, L.M.; Chiasson, J.N. DC-AC Cascaded H-Bridge Multilevel Boost Inverter with No Inductors for Electric/Hybrid Electric Vehicle Applications. *IEEE Trans. Ind. Appl.* **2009**, *45*, 963–970. [CrossRef]
65. Reimers, J.; Dorn-Gomba, L.; Mak, C.; Emadi, A. Automotive Traction Inverters: Current Status and Future Trends. *IEEE Trans. Veh. Technol.* **2019**, *68*, 3337–3350. [CrossRef]
66. Hofer Powertrain. Available online: https://www.hoferpowertrain.com/technology-page/hv-multi-level-inverter (accessed on 15 April 2023).
67. Abdelrahman, A.S.; Erdem, Z.; Attia, Y.; Youssef, M.Z. Wide Bandgap Devices in Electric Vehicle Converters: A Performance Survey. *Can. J. Electr. Comput. Eng.* **2018**, *41*, 45–54. [CrossRef]
68. Kumar, A.; Moradpour, M.; Losito, M.; Franke, W.T.; Ramasamy, S.; Baccoli, R.; Gatto, G. Wide Band Gap Devices and Their Application in Power Electronics. *Energies* **2022**, *15*, 9172. [CrossRef]

69. Song, Q.; Kozak, J.P.; Xiao, M.; Ma, Y.; Wang, B.; Zhang, R.; Volkov, R.; Smith, K.; Baksht, T.; Zhang, Y. Evaluation of 650V, 100A Direct-Drive GaN Power Switch for Electric Vehicle Powertrain Applications. In Proceedings of the IEEE 8th Workshop on Wide Bandgap Power Devices and Applications, WiPDA 2021, Crowne Plaza Redondo Beach and Marina, Los Angeles, CA, USA, 7–11 November 2021.
70. Husain, I.; Ozpineci, B.; Sariful Islam, M.; Member, S.; Gurpinar, E.; Member, S.; Su, G.-J.; Yu, W.; Chowdhury, S.; Xue, L.; et al. Electric Drive Technology Trends, Challenges, and Opportunities for Future Electric Vehicles. *Proc. IEEE* **2021**, *109*, 1039–1059. [CrossRef]